JOURNAL OF CATALYSIS **161,** 178–185 (1996)
ARTICLE NO. 0174

Promoter Effect of Sm_2O_3 on Ru/Al_2O_3 in Ammonia Synthesis

Yasushi Kadowaki and Ken-ichi Aika[1]

Department of Environmental Chemistry and Engineering, Interdisciplinary Graduate School of Science and Engineering, Tokyo Institute of Technology, 4259 Nagatsuta, Midori-ku, Yokohama 227, Japan

Received May 8, 1995; revised January 29, 1996; accepted January 30, 1996

Ammonia synthesis ($N_2 + 3H_2 = 80$ kPa) and the isotopic equilibration reaction (IER) of dinitrogen ($^{14}N_2 + {}^{15}N_2 = 20$ kPa) were studied on promoted and unpromoted Ru/Al_2O_3 catalysts around 588 K. Sm_2O_3 promoter was compared with CsOH promoter or the nonpromoted state. On the $Ru–Sm_2O_3/Al_2O_3$ catalyst, the ammonia synthesis rate was higher than the IER rate, whereas on the Ru/Al_2O_3 and $Ru–CsOH/Al_2O_3$ it was lower than the IER rate. For Ru/Al_2O_3 and $Ru–CsOH/Al_2O_3$ catalysts the IER rate was retarded by coexisting hydrogen. These results were explained with the Langmuir-type competitive adsorption model. Detailed kinetic parameters were obtained for Ru/Al_2O_3, where hydrogen adsorption ($Q_H = 9.9$ kcal mol^{-1}) was stronger than nitrogen adsorption ($Q_N = 4.2$ kcal mol^{-1}) with an activation energy of dissociative adsorption of N_2 14.3 kcal mol^{-1}. On the other hand, Sm_2O_3 released hydrogen poisoning against nitrogen adsorption. Hydrogen retardation was not observed in the IER on $Ru–Sm_2O_3/Al_2O_3$. The promotion by Sm_2O_3 was mainly due to hydrogen release, which might be related with the morphological modification of Ru by nascent Sm_2O_3. We also found that the $Ru–Sm_2O_3/Al_2O_3$ catalyst was active even under the high pressure ammonia synthesis condition due to the lesser hydrogen inhibition.

INTRODUCTION

One of the ruthenium catalysts has been used in a commercial ammonia plant since 1992 (1) after the use of iron catalysts since 1913. Ru is an excellent ammonia synthesis catalyst, especially when it is promoted with electron-donating or basic compounds (2). Based on this principle, several important factors were studied. Because chlorine acts as a poison, the precursor Ru compounds were recommended to be Chlorine-free (3–6). Promoter–Ru interaction was controlled by the preparation method, which decides the morphologic relationship between Ru and the promoter compounds (5, 6).

On the other hand, the activation of dinitrogen (the dissociative adsorption of dinitrogen) is retarded by hydrogen adsorption on Ru (7–9). Kinetic analysis of an isotopic equilibration reaction (IER) of nitrogen revealed that nitrogen and hydrogen were competing for the Ru surface site on Ru powder (8), Ru–K (7), $Ru–K/Al_2O_3$ (7), and Raney $Ru–CsNO_3$ (9). Hydrogen poisoning could be a serious problem with Ru catalysts used at high pressures under industrial conditions. The degree of hydrogen inhibition differs among the Ru catalysts and seems to depend on the nature of the support or promoter (5). Thus, many possibilities for improving the feature of the Ru catalyst with respect to getting rid of hydrogen poisoning may be available.

Recently, we found that lanthanide oxides are also effective promoters of Ru/Al_2O_3 as well as CsOH (5, 11). What is the role of the lanthanide oxide? Does it promote dinitrogen dissociation or does it release the hydrogen inhibition? To answer to these questions, ammonia synthesis and IER of nitrogen are compared on Ru/Al_2O_3, $Ru–CsOH/Al_2O_3$, and lanthanide promoted Ru/Al_2O_3. We selected Sm_2O_3 as a promoter among the lanthanide oxides.

Because the rate-determination step of ammonia synthesis is the dissociative adsorption of dinitrogen, the synthesis rate is a nitrogen dissociation rate in the presence of hydrogen. On the other hand, the rate of IER of nitrogen is the nitrogen dissociation rate without the presence of nitrogen. We can check hydrogen inhibition in this way.

EXPERIMENTAL

Catalyst Preparation

$Ru_3(CO)_{12}$ was used as a precursor of the Ru catalyst. This method has several advantages (4–6). First, the Ru particle can be highly dispersed on the support compared to the $RuCl_3$ precursor (4). The catalyst can be prepared free from chlorine ion, which acts as a poison. γ-Al_2O_3 (reference catalyst of Catalysis Society of Japan, JRC-ALO-4), which had been baked at 773 K, was impregnated with $Ru_3(CO)_{12}$ precursor at room temperature in tetrahydrofuran (THF). The Ru loading was 10 wt% as metal. After evaporation and drying, the sample was evacuated at 723 K for 2 h. Promoted catalysts were prepared by impregnation with aqueous samarium and cesium nitrate ($Sm(NO_3)_3$ and

[1] To whom correspondence should be addressed. E-mail: kenaika@chemenv.titech.ac.jp.

0021-9517/96 $18.00

$CsNO_3$, respectively) solution. A sample was dried at 373 K and reduced with hydrogen at 623 K in the reaction system shown below. Both promoters are believed to be turned into Sm_2O_3 (5) and CsOH (4), respectively. The molar ratios of promoter atom by Ru were 0.5 (Sm/Ru) and 1.0 (Cs/Ru), respectively.

Catalyst Characterization

The dispersion of Ru particle was measured by a volumetric method using hydrogen adsorption. The results are shown in Table 1. The amount of hydrogen adsorption was estimated from the adsorption isotherm of the Langmuir equation at 273 K. Here the hydrogen molecules are assumed to be adsorbed dissociatively on the Ru surface, but not on the support. The amount of Ru metal is expressed as the weight percentage (wt%). The amount of promoter is expressed as mole ratio against the amount of Ru.

Ammonia Synthesis and IER of Dinitrogen

Ammonia synthesis ($N_2 + 3H_2 \rightarrow 2NH_3$) and the IER ($^{15}N_2 + {}^{14}N_2 \rightarrow 2{}^{14}N{}^{15}N$) are performed in a conventional closed circulation system. Nitrogen and hydrogen gases were introduced by passing a liquid nitrogen trap to remove the condensable compound. In ammonia synthesis, formed ammonia is fixed in a liquid nitrogen trap. The rate of ammonia synthesis was measured by the volume decrease of $N_2 + 3H_2$ gas under constant pressure (80 kPa).

The IER of nitrogen was carried out under 20 kPa of $^{15}N_2 + {}^{14}N_2$ in a closed circulation system with a quadruple mass filter (AGA-100, ANELVA, Tokyo). The liquid nitrogen trap was not applied in this case. Reaction rates were calculated from the change of mole fraction of $^{14}N^{15}N$ with time. The rates of IER of nitrogen (R) were obtained from the equation

$$\ln[(X_e - X_t)/(X_e - X_i)] = -Rt/n, \qquad [1]$$

where X_e, X_t, and X_i are mole fraction of $^{14}N^{15}N$ at equilibrium, at time t, and at the beginning, respectively; n is the number of nitrogen molecules (12–14).

When the IER of nitrogen (20 kPa) is carried out under the presence of hydrogen (e.g., 4 kPa), very small amount of equilibrated ammonia (e.g., 16 Pa at 588 K) is also present. Under the synthesis condition, N_2(20 kPa) + $3H_2$(60 kPa) gas gives about 920 Pa (1.15%) of equilibrium NH_3 at 588 K, however, N_2(20 kPa) + $0.2H_2$(4 kPa) gas (IER condition) gives only 16 Pa of equilibrium NH_3. The catalysts used here shows the activity level of 0.1 mmol/h/g (0.068% or 54 Pa of NH_3 partial pressure at the outlet) under 60 mlSTP/min of $N_2 + 3H_2$ gas flow. The partial pressure of produced ammonia is about 6% of the equilibrium value under the synthesis condition; however, it exceeds (more than three times) the equilibrium under the IER condition (if the synthesis rate is not changed by the hydrogen pressure). This means that the equilibrium concentration of ammonia passes throuh the closed circulation system (ca. 180 ml) in 3 min. Thus, ammonia formation does not practically proceed during the IER run.

The rate of ammonia synthesis and IER were expressed by turnover frequency of nitrogen (TOF; N_2 molecule site^{-1} s^{-1}). In the case of ammonia synthesis, formation of two ammonia molecules is counted as one reaction.

High Pressure Ammonia Synthesis

A stainless steel high pressure flow reaction system was used. This system can be operated at a temperature and pressure up to 673 K and 50 kg/cm^2. $N_2 + 3H_2$ (ratio of 1 : 3) gas was supplied from the cylinder without purification. No catalyst deactivation was observed during the synthesis for several days in any catalysts studied here. The ammonia synthesis rate was determined by the decreased rate of electron conductivity of diluted sulfuric acid solution, which fixed the produced ammonia (3, 8).

TABLE 1

Properties of Ru Catalysts

Catalyst name	Ru loading (wt %)	Promoter loading (M/Ru mol ratio)	H_2 uptake at 273 K (ml/g)	Dispersion (H/Ru total)
Ru/Al_2O_3	10	0	2.84	0.26
$Ru–CsOH/Al_2O_3$	10	1.0	2.28	0.21
$Ru–Sm_2O_3/Al_2O_3$	10	0.5	2.72	0.24

RESULTS

Ammonia Synthesis and IER of Dinitrogen on Ru/Al_2O_3 and $Ru–CsOH/Al_2O_3$

The Arrhenius plot of ammonia synthesis (the rate of dissociative adsorption of nitrogen with hydrogen) and IER of nitrogen (the rate of dissociative adsorption of nitrogen free from hydrogen) on Ru/Al_2O_3 and $Ru–CsOH/Al_2O_3$ are shown in Figs. 1 and 2 respectively. The apparent activation energies and TOFs at 588 K are shown in Table 2. As shown in Figs. 1 and 2, the ammonia synthesis rates over the unpromoted catalyst (Ru/Al_2O_3) and the cesium-promoted catalyst ($Ru–CsOH/Al_2O_3$) were slower than the IER rates. Similar results have been shown for Raney Ru and $Ru–CsNO_3$ (9), where the rate ratios of IER (N_2 mmol h^{-1} g^{-1})/synthesis ($0.5 \times NH_3$ mmol h^{-1} g^{-1}) at 573 K are 0.17/0.04 and 14.7/1.37, respectively.

In IER, the nitrogen adsorption keeps an equilibrium between the surface and gas phase and the Ru surface is covered with atomic nitrogen alone (9, 15). On the other hand, in the ammonia synthesis reaction, the atomic nitrogen on

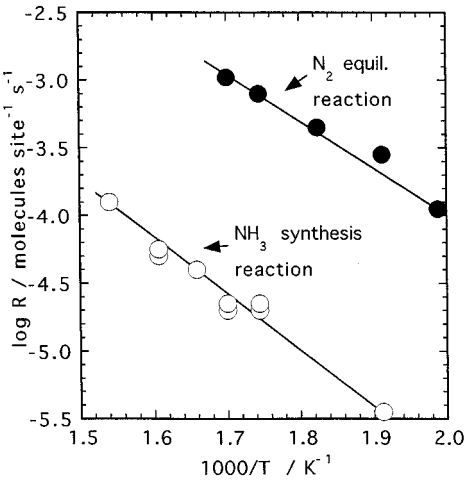

FIG. 1. Arrhenius plots of ammonia synthesis rate ($N_2+3H_2=$ 600 Torr, open circles) and isotopic equilibration reaction rate of nitrogen ($^{15}N_2+{}^{14}N_2=150$ Torr, closed circles) on 10% Ru/Al_2O_3. Conversion rates of N_2 molecules are compared for both reactions.

the Ru surface is rapidly hydrogenated and removed under a dynamic state (2). Furthermore, nitrogen and hydrogen are competitively adsorbed on the Ru surface in ammonia synthesis. If hydrogen adsorption is much stronger than nitrogen adsorption, the Ru surface would be almost covered with the hydrogen atoms. Actually, it is generally considered that hydrogen inhibits the nitrogen activation process on Ru, hydrogen poisoning (7, 8, 13, 16). In this case, ammonia synthesis is slower than the IER (Ru/Al_2O_3, $Ru–CsOH/Al_2O_3$).

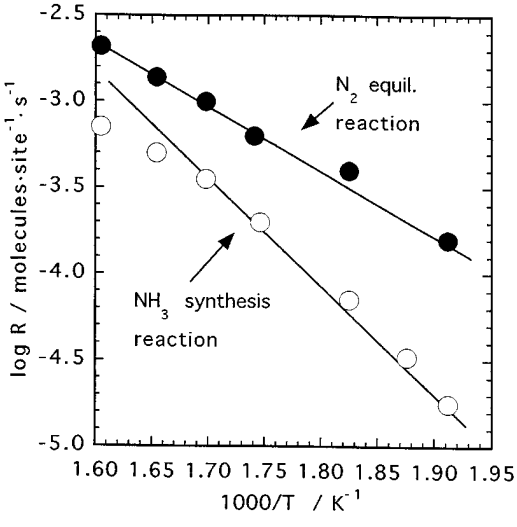

FIG. 2. Arrhenius plots of ammonia synthesis rate ($N_2+3H_2=600$ Torr, open circles) and isotopic equilibration reaction rate of nitrogen ($^{15}N_2+{}^{14}N_2=150$ Torr, closed circles) on 10% $Ru–CsOH/Al_2O_3$ (Cs/Ru = 1/1 (mol/mol)). Conversion rates of N_2 molecules are compared for both reactions.

TABLE 2

Rate Data of Ammonia Synthesis and Isotopic Equilibration Reaction of N_2 on Three Ru Catalysts

	NH_3 synthesis[a]		IER of N_2[b]	
Catalysts	E_a (kcal/mol)	TOF at 588 K (site^{-1} s^{-1} × 10^4)	E_a (kcal/mol)	TOF at 588 K (site^{-1} s^{-1} × 10^4)
Ru/Al_2O_3	15.1	0.27	14.8	6.29
$Ru–CsOH/Al_2O_3$	27.7	1.89	15.9	9.57
$Ru–Sm_2O_3/Al_2O_3$	16.5	1.34	23.5	0.60

[a] N_2 150 Torr, H_2 459 Torr.
[b] N_2 150 Torr.

Effects of Hydrogen on the IER of Nitrogen over Ru/Al_2O_3, Derivation of Competitive Adsorption Parameters

The ammonia synthesis and IER rate are not the same even on an identical catalyst. Several explanations may be proposed. The hydrogen coexistence may change the nature of the surface or simply occupy the nitrogen adsorption site on the Ru surface. To clarify these phenomena, hydrogen pressure dependence and nitrogen pressure dependence of the IER were investigated.

The simple model was assumed. The adsorbed hydrogen and nitrogen were competing with each other to occupy the same site (Ru surface). Under the equilibrium of two adsorption processes, the coverages of N(a) and H(a) are represented as a function of pressures according to the Langmuir equation.

$$N_2 + 2\ \text{sites} = 2N(a) \qquad [2]$$

$$H_2 + 2\ \text{sites} = 2H(a). \qquad [3]$$

As is stated under experimental, ammonia production can be ignored because of the equilibrium consideration under the IER run. The rates of dissociative adsorption (R_a) and desorption (R_d) of nitrogen are expressed as (7, 14)

$$R_a = k_a P_{N_2}(1-\Theta_N-\Theta_H)^2 \qquad [4a]$$

$$R_d = k_d \Theta_N{}^2, \qquad [4b]$$

where k_a and k_d are the adsorption and desorption rate constants, respectively. Under the equilibrium condition, R_a equals R_d, giving the following relation:

$$(K_N P_{N_2})^{0.5} = \Theta_N/(1-\Theta_N-\Theta_H). \qquad [5]$$

The similar relation about the hydrogen adsorption is obtained as

$$(K_H P_{H_2})^{0.5} = \Theta_H/(1-\Theta_N-\Theta_H), \qquad [6]$$

where K_N ($=k_a/k_d$) and K_H are the adsorption equilibrium constants, Θ_N and Θ_H are the coverages, and P_{N_2} and P_{H_2} are

the pressures. $(1-\Theta_H-\Theta_N)$ means density of unoccupied site on the Ru surface.

It should be noted that R obtained from Eq. [1] (the IER rate), is identical to the forward rate of dissociative adsorption under the equilibrium, R_a $(= R_d)$, because the dissociative adsorption causes atomic randomization of dinitrogen. Thus, from Eqs. [4], [5], and [6], Eq. [7] is obtained,

$$R^{-0.5} = (k_a P_{N_2})^{-0.5} + (K_N/k_a)^{0.5} + (K_H P_{H_2}/k_a P_{N_2})^{0.5}, \quad [7]$$

where R means R_a $(= R_d)$, which equals to the IER rate. It is to be noted that the net rate of adsorption, R_a–R_d, is null here.

The IER rate was measured on Ru/Al_2O_3 under the existence of hydrogen of various pressures at various temperatures. Under these conditions, all the processes such as nitrogen adsorption–desorption, hydrogen adsorption–desorption, and ammonia synthesis–decomposition are in equilibrium. Produced ammonia is not being fixed in a trap but circulated as a gas with the equilibrium content below 1%. Figure 3 shows the rate of IER as a function of hydrogen pressure. Nitrogen activation was retarded by the hydrogen pressure increase. These data are rearranged in $R^{-0.5}$ vs $P_{H_2}^{0.5}$ plot as is shown in Fig. 4.

With the absence of hydrogen, Eq. [7] turns into

$$R^{-0.5} = (k_a P_{N_2})^{-0.5} + (K_N/k_a)^{0.5}. \quad [8]$$

The IER rates without hydrogen were measured as a function of P_{N_2} on Ru/Al_2O_3 at various temperatures. The data were rearranged in Fig. 5 in the form of Eq. [8]. The slope gives k_a, and the intercept at zero of $P_{N_2}^{-0.5}$ gives K_N. The K_a and K_N slopes are shown in Fig. 6. Thus, these constants are put into Eq. [7]. Now, Eq. [7] can be fitted to Fig. 4: $R^{-0.5}$ vs $P_{H_2}^{0.5}$ plots. The slope gives K_H, which is shown also in Fig. 6.

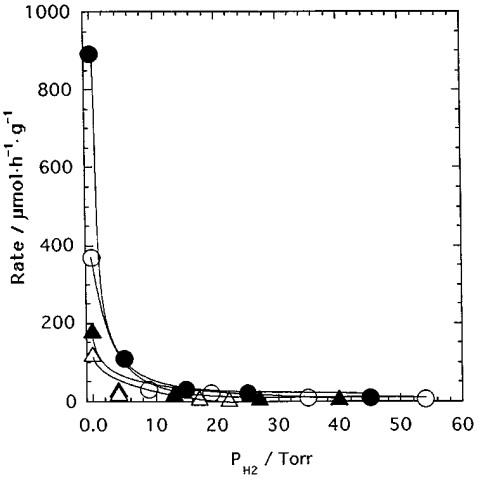

FIG. 3. Rate of nitrogen isotopic equilibration reaction on 10% Ru/Al_2O_3 under 150 Torr of $^{15}N_2 + {}^{14}N_2$ as a function of hydrogen pressure at various temperatures (△ 573 K, ▲ 588 K, ○ 603 K, and ● 623 K).

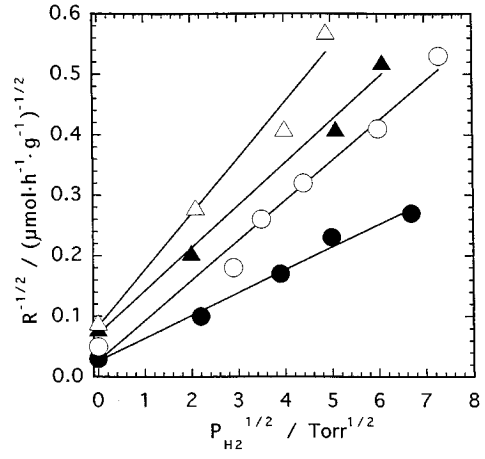

FIG. 4. Plot of $R^{-0.5}$ as a function of $P_{H_2}^{-0.5}$ (see Eq. [7]) at various temperatures (△ 573 K, ▲ 588 K, ○ 603 K, and ● 623 K) under 150 Torr of $^{15}N_2 + {}^{14}N_2$. R, rate of isotopic equilibration reaction of nitrogen on 10% Ru/Al_2O_3.

The competitive adsorption model explains the hydrogen retardation against nitrogen activation or IER of nitrogen.

The activation energy and the heat of adsorption of nitrogen and hydrogen are obtained from the change of k_a, K_N, and K_H as a function of temperature (Fig. 6). The relationship between reaction rate constants and temperature are shown as

$$\ln(k_a) = \ln(A) - E_a/RT, \quad [9]$$

where E_a is the activation energy of adsorption and A is the frequency factor. The Arrhenius plot in Fig. 6 gives the value of E_a as 14.3 kcal/mol. A similar relation is known

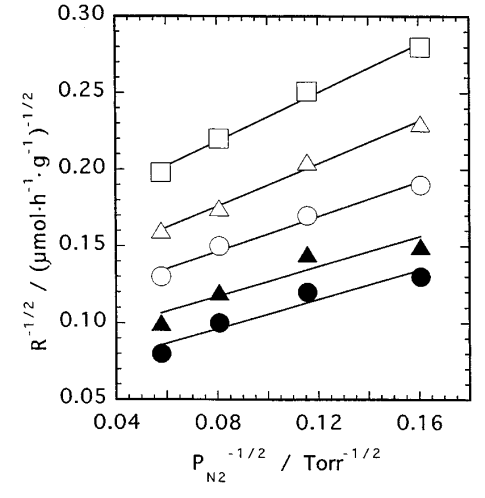

FIG. 5. Plot of $R^{-0.5}$ as a function of $P_{N_2}^{-0.5}$ (see Eq. [8]) at various temperatures (□ 558 K, △ 573 K, ○ 588 K, ▲ 603 K, and ● 623 K) under 150 Torr of $^{15}N_2 + {}^{14}N_2$. R, rate of isotopic equilibration reaction of nitrogen on 10% Ru/Al_2O_3.

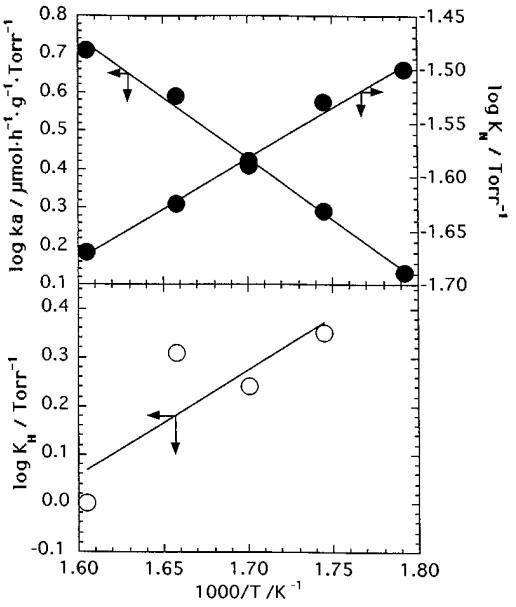

FIG. 6. Arrhenius plot of k_a, K_N, and K_H which were determined from Eqs. [7] and [8] (Figs. 4 and 5) for IER of N_2 with or without hydrogen on 10% Ru/Al_2O_3.

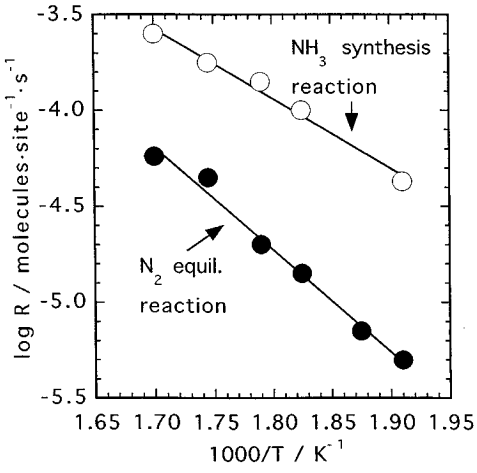

FIG. 7. Arrhenius plots of ammonia synthesis rate ($N_2 + 3H_2 = 600$ Torr, open circles) and isotopic equilibration reaction rate of nitrogen ($^{15}N_2 + {}^{14}N_2 = 150$ Torr, closed circles) on 10% $Ru–Sm_2O_3/Al_2O_3$ ($Sm/Ru = 1/2$ (mol/mol)). Conversion rates of N_2 molecules are compared for both reactions.

between adsorption constant and temperature,

$$\ln(K_N) = \ln(C) + Q_N/RT, \qquad [10]$$

where Q_N is the heat of adsorption of nitrogen and C is the constant. The plot in Fig. 6 gives the heat of nitrogen adsorption (Q_N) as 4.2 kcal/mol. Figure 6 gives the heat of hydrogen adsorption (Q_H) as 9.9 kcal/mol. Thus, in unpromoted catalyst (Ru/Al_2O_3), the heat of hydrogen adsorption is higher than the heat of nitrogen adsorption. These parameters are shown in Table 3 together with the reported values.

Ammonia Synthesis and IER of Nitrogen on $Ru–Sm_2O_3/Al_2O_3$

The rates of ammonia synthesis and IER of nitrogen were measured on $Ru–Sm_2O_3/Al_2O_3$ at various temperatures. The results are shown as Arrhenius plots in Fig. 7. Interestingly, for samarium-promoted catalyst ($Ru–Sm_2O_3/Al_2O_3$), the ammonia synthesis rate is faster than the IER rate, contrary to the case of Ru/Al_2O_3 or $Ru–CsOH/Al_2O_3$. However, this is natural if hydrogen does not retard the nitrogen activation, because the dynamic process (ammonia synthesis) is faster (in a free energy cascade) than the forward and backward reaction in the equilibrium (IER, no free energy cascade). Here, Sm_2O_3 promoter causes release of hydrogen poisoning on the Ru surface. Thus, the effect of hydrogen on IER of nitrogen was studied.

Effect of Hydrogen on the IER over $Ru–Sm_2O_3/Al_2O_3$

The rate of IER of 150 Torr N_2 was measured as a function of hydrogen pressure over $Ru–Sm_2O_3/Al_2O_3$. Reference data were taken over Ru powder. The results are shown in Fig. 8 together with data on Ru/Al_2O_3. Although the IER rate was drastically inhibited by the coexistence of hydrogen on Ru powder or Ru/Al_2O_3, it was not retarded by the addition of hydrogen over the Sm_2O_3 promoted catalyst. Nitrogen activation even seems to be promoted by hydrogen

TABLE 3

Kinetic Parameter of IER of N_2 in the Presence of H_2

	E_a (kcal mol^{-1})	E_{app}[a] (kcal mol^{-1})	Q_N (kcal mol^{-1})	Q_H (kcal mol^{-1})	Ref.
Ru/Al_2O_3	14.3	14.8	4.2	9.9	This work
Ru–K[b]	14	32	40	—	14
$Ru–K/Al_2O_3$[b]	10	25	22	—	14
Raney–$CsNO_3$	15.0	22	11.6	19.3	9

[a] Apparent activation energy.
[b] Hydrogen effect has not been studied.

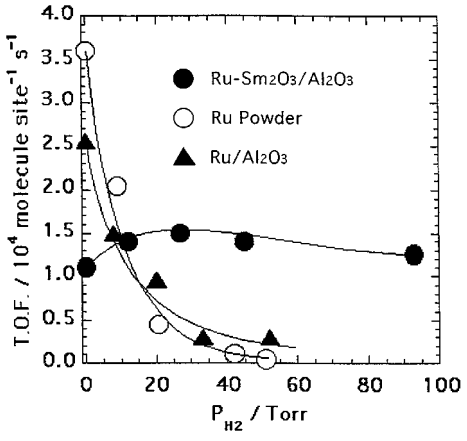

FIG. 8. Rates of nitrogen isotopic equilibration reaction under 150 Torr of $^{15}N_2 + {}^{14}N_2$ on Ru powder, 10% $Ru–Al_2O_3$, and 10% $Ru–Sm_2O_3/Al_2O_3$ (Sm/Ru = 1/2 (mol/mol)) as a function of hydrogen pressure at 588 K.

at low pressure. Now, it is clear that hydrogen inhibition was not found on Sm_2O_3 added Ru surface. Sm_2O_3 seems to change the nature of the Ru surface mainly with respect to hydrogen inhibition.

Ammonia Synthesis in a High Pressure Flow System

It is important to investigate how these catalysts behave under high pressure, because the industrial ammonia synthesis is carried out under high pressure. The ammonia synthesis rate was measured at various pressures up to 30 or 40 atm for $Ru–Sm_2O_3/Al_2O_3$ and $Ru–CsOH/Al_2O_3$ at 588 K. The results are shown in Fig. 9. For the $Ru–CsOH/Al_2O_3$ catalyst, the rate even decreases as the total pressure increases. However, for the $Ru–Sm_2O_3/Al_2O_3$ catalyst, the rate increases as the pressure increases. Thus,

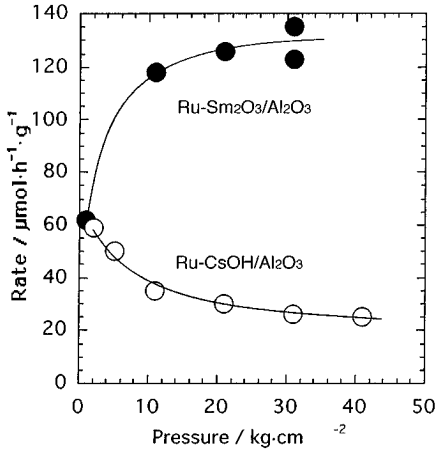

FIG. 9. Rates of high pressure ammonia synthesis on 10% $Ru–Sm_2O_3/Al_2O_3$ (Sm/Ru = 1/2 (mol/mol)) and 10% Ru–CsOH/Al pressure ($N_2 + 3H_2$) at 588 K.

$Ru–CsOH/Al_2O_3$ and $Ru–Sm_2O_3/Al_2O_3$ show completely different behaviors of pressure dependence due to the kind of promoter. Although $Ru–CsOH/Al_2O_3$ loses ammonia activity due to hydrogen inhibition at high pressure, $Ru–Sm_2O_3/Al_2O_3$ catalyst is active even under the high pressure condition. From these results, it seems that the promotion effect of Sm_2O_3 in ammonia synthesis is mainly due to releasing hydrogen poisoning for the activation of nitrogen.

DISCUSSION

Hydrogen Effect on N_2 Activation over Ru Catalysts

The possible causes of hydrogen effect are summarized in Table 4. The simplest model is the competitive adsorption of nitrogen and hydrogen(1.1), where the electronic state of Ru surface is not assumed to be changed by hydrogen adsorption. Detailed kinetic work has been done on Ru powder (8) and Raney $Ru–CsNO_3$ (9). The same model (Eqs. [1] to [8]) was used in this study to analyze the IER of nitrogen on Ru/Al_2O_3. The hydrogen retarding effect was, thus, explained by this model, where heat of hydrogen adsorption was higher than the heat of nitrogen adsorption. Kinetic parameters of IER of nitrogen are shown in Table 3. The activation energy of dissociative adsorption of nitrogen (E_a) ranges from 10 to 15 kcal mol^{-1} on four kinds of Ru catalyst. Their apparent activation energies (E_{app}) are higher than their E_a, because those must be the sum of E_a and a part of Q_N. The heat of nitrogen adsorption (Q_N) on Ru/Al_2O_3 is somehow lower than those on the other Ru catalysts. The heat of hydrogen adsorption (Q_H) is higher than Q_N both in Ru/Al_2O_3 and Raney $Ru–CsNO_3$.

The same model was applied for Ru–K (7) where the two rate equations were determined independently for the hydrogen system and for the hydrogen-free system. The rate constant of nitrogen adsorption itself was smaller when hydrogen was introduced, suggesting that hydrogen adsorption modifies Ru surface or induced effect of hydrogen adsorption (1.2). Recently adsorbed dinitrogen (17) and

TABLE 4

Possible Causes of Hydrogen Effect on N_2 Activation over Ru Catalysts

Classification	Reference
1. Nonstructural change (reversible)	
1.1. Competitive adsorption of N_2 and H_2	7–10
1.2. Induced effect of hydrogen adsorption	7, 18
1.3. Change of main adsorbed species (such as N to NH)	2, 9
2. Reversible structural change	
2.1. Ru: Sublayer hydride formation	19
2.2. Promoter or Support: Reversible surface hydroxide formation	20
2.3. Ru-support interface: Hydrogen bridge formation	21, 28

hydrogen atoms (18) were successfully identified by FTIR at room temperature. The dinitrogen adsorption process was found to be retarded by hydrogen atom adsorption on Ru/MgO or Ru–CsOH/MgO, where short-range or long-range interaction between N_2(a) and H(a) are suggested (18). This kind of effect must be important especially for the phenomena at low temperature; however, it is difficult to conclude this effect from the kinetic data at high temperature because the accuracy or amount of kinetic data did not permit determination of two kinds of rate constant with and without hydrogen. To conclude, there may be two causes (1.1 and 1.2) for hydrogen retardation; however, a simple competitive adsorption model (1.1) is enough to explain it at present.

With iron catalyst, hydrogen promotes nitrogen activation (2), where the induced effect (1.2) and the change of adsorbed species from N to NH (1.3) are suggested. As for Ru catalysts, this term usually is not important in the kinetic expression (10).

Recent works have disclosed several structural changes due to hydrogen. Hydrogen atom can be incorporated under the outermost layer of Ru surface (19). This may cause loosening of surface Ru atoms which may further change the nature of nitrogen activation (2.1). Over $Pt/SO_4^{2-}–ZrO_2$, spilled over hydrogen is suggested to be turned to surface proton and bulk electron (20). On the Ru–support system, too, spillover hydrogen may change the nature of support (2.2). If a Pt particle is small on Al_2O_3, hydrogen is said to be located on the interface between Pt and oxide (21). If this case occurs in the Ru–support system, the nature of Ru might be changed (2.3). These structural changes may be reversible at least in a long time scale. These effects must be studied in the future.

Promotor and Support Dependency of Hydrogen Adsorption

As has been discussed above, several factors should be considered; however, strong hydrogen adsorption must be the decisive factor to retard the nitrogen activation on Ru-powder (8, this study), Ru/Al_2O_3 (this study), $Ru–CsOH/Al_2O_3$ (this study), Ru–K (7), and Raney Ru–$CsNO_3$ (9). The degree of hydrogen adsorption and nitrogen adsorption during ammonia synthesis has been evaluated (10). The degree depends on the support and promoter. However, the authors could not foretell that Sm_2O_3 could release hydrogen poisoning on Ru/Al_2O_3.

Promoter Effect: Electronic, Morphology, and Hydrogen Release

Ammonia synthesis is a well known structure sensitive reaction which has been studied on iron single crystals. However, this reaction seems more sensitive to electronic state of active site if it runs on Ru (1). Ruthenium catalysts have been proven to be sensitive to the nature of the support and of the promoter (1). Compounds that have electron-donating or basic properties have been reported to be effective promoters (4–7, 22–25). The effectiveness of a promoter or support is roughly related to the electronegativity of the compound (e.g., Cs > K > Na > CsOH > KOH > NaOH = CaO = SrO > MgO > Sm_2O_3 > Al_2O_3) (6, 25) (electronic).

Alkaki, an electron-donating compound, is considered to donate electrons to Ru surface, where dinitrogen is activated effectively and N–N stretching frequency of adsorbed dinitrogen on Ru is shifted to a lower wave number when alkali is added or the Al_2O_3 support is replaced with MgO support (17). IEA of N_2 is accelerated by adding K to Ru (24) or by adding CsOH (Table 2). However, Alkali does not seem to release the strong hydrogen adsorption. On the other hand, lanthanide oxides do not seem to donate enough electrons so that IEA of N_2 is not accelerated by adding it (Sm_2O_3 in Table 2 and Fig. 8). Instead, Sm_2O_3 was found in this study to release hydrogen so that ammonia synthesis was promoted. We tentatively suppose that lanthanide oxide can release strong hydrogen inhibition by modifying Ru surface atoms morphologically as follows. When Al_2O_3 is used as a support, much $CsNO_3$ precursor is necessary to get enough activity in ammonia synthesis. This is because the CsOH may be consumed for the neutralization of acidic sites on the Al_2O_3 surface. However, when $Sm(NO_3)_3$ was used as a precursor, a smaller amount of it compared to CsOH was effective (5). Because the melting point of Sm_2O_3 is very high (2573 K), Sm_2O_3 formed on the Ru particle may not spread easily to the support because of its low mobility (morphology). Some of the Sm_2O_3 is considered to be left on the Ru surface like in the decolation model in SMSI phenomena of Pd/La_2O_3 (26, 27). The intimate interaction between the nascent Sm_2O_3 and Ru surface atoms might cause the hydrogen adsorption to be weaken. Recently, several studies have reported the interaction between SMSI oxide and transition metal (21, 28). These studies have been performed with *in situ* extended X-ray absorption fine structure. For example, direct bonding between Rh and Ta^+ cation of the oxide has been proposed in the SMSI state for the Rh/Ta_2O_5 catalyst. Such a state might occur for the $Ru–Sm_2O_3$ system, which has been prepared from $Ru–Sm(NO_3)_3$. This assumption must be tested in the future.

CONCLUSION

In the Ru/Al_2O_3 and $Ru–CsOH/Al_2O_3$ catalyst, IER is strongly poisoned by hydrogen. The ammonia synthesis rate is lower than the IER rate by an order of magnitude. These behaviors have been reported for the other Ru catalyst, for example, Raney Ru (9), Ru–K/A.C. (13), and $Ru–K/Al_2O_3$ (7). The retardation of nitrogen activation with hydrogen on these catalysts was thought to be due to

stronger adsorption of hydrogen than nitrogen. The retardation of nitrogen activation with hydrogen on Ru/Al_2O_3 catalyst has also been explained by competitive adsorption. The variation of IER rate as a function of hydrogen partial pressure was explained by the Langmuir-type competitive adsorption model. The adsorption energy of hydrogen was larger than the nitrogen adsorption energy. This result is reasonable for the hydrogen poisoning of nitrogen activation.

However, for $Ru–Sm_2O_3/Al_2O_3$, the hydrogen retardation was not observed. It was proved by the comparison of synthesis rate and IER rate and by the lack of hydrogen effect on IER. $Ru–Sm_2O_3/Al_2O_3$ is not retarded extensively by hydrogen even in the high pressure condition. Thus, we could control the hydrogen effect by applying lanthanide oxides on the ruthenium catalyst. Sm_2O_3 is one candidate for the promoter of ruthenium ammonia synthesis catalyst for the next generation.

REFERENCES

1. Chem. Engineering, March 1993, p. 19, Chementator; Czuppou, T. A., Knez, S. A., Schneider, R. V., III, and Worobets, G., presented at the 1993 American Institute of Chemical Engineers, Ammonia Safty Symposium, September 1993, Orlando, FL.
2. Ozaki, A., Aika, K., "Catalysis—Science and Technology" (J. R. Anderson, and M. Boudart, Eds.), Vol. 1, Chap 3, p. 87. Springer-Verlag, Berlin/Heidelberg, 1981.
3. Murata, S., and Aika, K., *Appl. Catal. A.* **82**, 1 (1992).
4. Murata, S., and Aika, K., *J. Catal.* **136**, 110 (1992).
5. Murata, S., and Aika, K., *J. Catal.* **136**, 118 (1992).
6. Aika, K., Takano, T., and Murata, S., *J. Catal.* **136**, 126 (1992).
7. Urabe, K., Aika, K., and Ozaki, A., *J. Catal.* **42**, 197 (1976).
8. Rambeau, G., and Amariglio, H., *J. Catal.* **72**, 1 (1981).
9. Hikita, T., Kadowaki, Y., and Aika, K., *J. Phys. Chem.* **95**, 9396 (1991).
10. Aika, K., Kumasaka, M., Oma, T., Kato, O., Matsuda, H., Watanabe, N., Yamazaki, K., Ozaki, A., and Onishi, T., *Appl. Catal.* **28**, 57 (1986).
11. Murata, S., Aika, K., and Onishi, T., *Chem. Lett.* 1067 (1990).
12. Morikawa, Y., and Ozaki, A., *J. Catal.* **12**, 145 (1968).
13. Urabe, K., Aika, K., and Ozaki, A., *J. Catal.* **32**, 108 (1974).
14. Urabe, K., Aika, K., and Ozaki, A., *J. Catal.* **38**, 430 (1975).
15. Ogata, Y., Aika, K., and Onishi, T., *Chem. Lett.* 825 (1984).
16. Guyer, W. R., Joris, G. G., and Taylor, H. S., *J. Chem. Phys.* **9**, 287 (1941).
17. Kubota, J., and Aika, K., *J. Phys. Chem.* **98**, 11293 (1994).
18. Izumi, Y., Hoshikawa, M., and Aika, K., *Bull. Chem. Soc. Jpn.* **67**, 3191 (1994).
19. Yates, J. T., Jr., Peden, C. H. F., Houston, J. E., and Goodman, D. W., *Surf. Sci.* **160**, 37 (1985).
20. Ebitani, K., Konno, H., Tanaka, T., and Hattori, H., *J. Catal.* **135**, 60 (1992).
21. Martens, J. H. A., Prins, R., and Koningsberger, D. C., *Catal. Lett.* **2**, 211 (1989).
22. Aika, K., Hori, H., and Ozaki, A., *J. Catal.* **27**, 424 (1972).
23. Aika, K., Shimazaki, K., Hattori, Y., Ohya, A., Ohshima, S., Shirota, K., and Ozaki, A., *J. Catal.* **92**, 296 (1985).
24. Aika, K., Kawahara, T., Murata, S., and Onishi, T., *Bull. Chem. Soc. Jpn.* **63**, 1221 (1990).
25. Aika, K., Ohya, A., Inoue, Y., and Yasumori, I., *J. Catal.* **92**, 305 (1985).
26. Tauster, S. T., *Acc. Chem. Res.* **20**, 389 (1987).
27. Fleisch, T. H., Hicks, R. F., and Bell, A. T., *J. Catal.* **87**, 398 (1984).
28. Koningsberger, D. C., Martens, J. H. A., Prins, R., Short, D. R., and Sayers, D. E., *J. Phys. Chem.* **90**, 3047 (1986).